

# Microstructural analysis of selective C/Al<sub>2</sub>O<sub>3</sub>/Al solar absorber surfaces

P. Konttinen<sup>a,\*</sup>, R. Kilpi<sup>b</sup>, P.D. Lund<sup>a</sup>

<sup>a</sup>Advanced Energy Systems Laboratory, Helsinki University of Technology, P.O. Box 2200, FIN-02015 HUT, Finland

<sup>b</sup>Shield Ltd, P.O. Box 204, FIN-00151 Helsinki, Finland

Received 8 April 2002; received in revised form 27 November 2002; accepted 5 December 2002

## Abstract

The elemental composition and geometrical structure of mechanically manufactured spectrally selective C/Al<sub>2</sub>O<sub>3</sub>/Al solar absorber surfaces were characterized by X-ray photoelectron spectroscopy (XPS), scanning electron microscopy, energy dispersive X-ray spectroscopy and optical microscopy. The XPS analysis revealed that the surface contains Al<sub>2</sub>O<sub>3</sub> and C in graphite form. Optical microscopy confirmed that graphite forms inhomogeneous agglomerated clusters on the surface. The thickness of the clusters varies, the maximum measured thickness being in the range of 300 nm. A solar absorptance of 0.90 and a thermal emittance of 0.22 have been achieved so far. Increasing the graphite coverage and decreasing the graphite cluster thickness could increase the absorptance to  $\geq 0.94$  and lower the emittance. This could be achieved by altering the composition and the structure of the grinding pad used and by finding the suitable manufacturing parameters for the advanced pad.

© 2002 Elsevier Science B.V. All rights reserved.

**Keywords:** Aluminium oxide; Graphite; Optical coatings; Scanning electron microscopy

## 1. Introduction

Spectrally selective solar surfaces are used for conversion of solar radiation into thermal energy. Today's state-of-the-art selective solar surfaces are mainly manufactured by sputtering and have good optical properties: hemispherical solar absorptance:  $90\% < \alpha < 99\%$  and hemispherical thermal emittance (at 100 °C):  $2\% < \varepsilon < 10\%$  [1–4]. Some older technologies are becoming obsolete mainly due to environmental reasons; for example electroplating produces large quantities of chemical waste. However, sputtering may require high investments in the manufacturing technology, thus making the resulting surfaces expensive. Alternative lower-cost manufacturing methods are being developed, such as selective paints [5,6]. Another method for a low-cost mass-production of selective surfaces can be mechanical manufacturing.

An early work on using mechanical grinding to increase the selectivity of surfaces prior to deposition of multilayer interference coating has been reported by

Kudryashova [7]. His approach was to manufacture copper or duralumin surfaces with a uniform distribution of irregularities with a depth of a few microns in order to achieve optical trapping of solar radiation by multiple reflections on the surface. After cleaning and polishing with chromium oxide paste, he grinded the specimens for 10–15 min using different micropowders. The best results for duralumin were achieved with diamond powder (grain size 1  $\mu\text{m}$ ):  $\alpha = 0.68$ ,  $\varepsilon = 0.06$ . The best  $\alpha$  was 0.73 ( $\varepsilon = 0.29$ ) by using boron carbide powder (grain size 30  $\mu\text{m}$ ). Results for copper plates were in the same range. No particulate coating (e.g. graphite) was added in the grinding process.

Development of manufacturing processes and durability testing of mechanically manufactured selective C/Al<sub>2</sub>O<sub>3</sub>/Al surface has been reported by Konttinen et al. [8] and Konttinen [9]. In this paper the C/Al<sub>2</sub>O<sub>3</sub>/Al surface is analysed by X-ray photoelectron spectroscopy (XPS), scanning electron microscopy (SEM), energy dispersive X-ray spectroscopy (EDS) and optical microscopy. Experimental results on the influence of varying manufacturing parameters on the absorptance and emittance of the surface are described.

\*Corresponding author. Tel.: +358-9-4513212; fax: +358-9-4513195.

E-mail address: [petri.konttinen@hut.fi](mailto:petri.konttinen@hut.fi) (P. Konttinen).

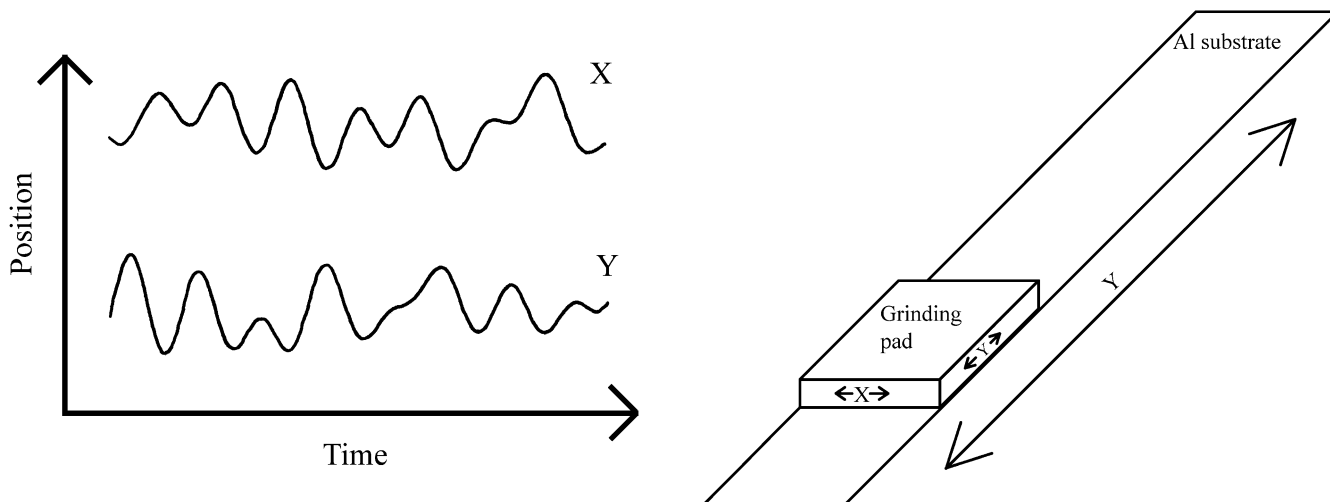


Fig. 1. The non-correlating classical random noise used for moving the grinding pad in  $X/Y$ -directions across the substrate (left and right). The substrate moves back and forth slowly in  $Y$ -dimension (right, not on scale).

## 2. Manufacturing principle of the selective $C/Al_2O_3/Al$ surface

Spectrally selective  $C/Al_2O_3/Al$  surfaces can be manufactured with several different processes [8]. In the latest version the surfaces were manufactured on Al-substrate sheets by mechanically operated grinding. The dimensions of the 99.5% pure Al-substrate sheets are: length 2 m, width 0.12 m and thickness 0.5 mm. The mechanical grinding method implements a non-correlating classical random noise signal, which generates the control voltage for the  $X/Y$ -electromagnetic control units of the grinding unit. The grinding unit drives a grinding pad attached to a wheel head (Fig. 1). Very hard grinding particles, e.g. silicon carbide are attached in the pad thus forming a three-dimensional matrix. The size of the particles varies and is typically between 300 nm and 2  $\mu\text{m}$ . While the pad wears, new particles come into touch with the surface of the absorber substrate, increasing the uniformity of the process. The Al-substrate sheet moves back and forth under the grinding unit in a relatively slow motion, typically less than 1  $\text{m s}^{-1}$ . In addition, the grinding unit moves the grinding pad across the substrate two-dimensionally with variable speed (from 0 to 20  $\text{m s}^{-1}$ ) and direction.

During the grinding process the grinding pad is saturated with carbon dust, which is bound to the pad by static electricity. Carbon dust reacts with the surface being scratched (containing  $Al_2O_3$  and unoxidized Al) and atmospheric oxygen forming a matrix structure on the final surface. This structure contains mainly elements Al, O and C [8], and it covers the surface as a black or dark grey layer. Changing the size of the grinding particles, grinding pressure, speed and time has strong effect on the optical properties of the forming surface.

## 3. Results

Surfaces were characterized by optical microscopy (Nikon type 104 equipped with a JVC 3-CCD colour video camera, model KY-F55B), XPS (Surface Science Instruments, model SSX-100), SEM (model JEOL JSM-820) and field emission SEM (model DSM 982 Gemini).

### 3.1. Optical microscopy analysis

A typical surface (denoted as F) manufactured by 15 min of mechanical grinding was examined by optical microscopy. The measured optical properties of the surface F are: the (AM 1.5) solar absorptance  $\alpha$  is 0.88 and the thermal emittance  $\varepsilon$  is 0.27 (at 100  $^\circ\text{C}$ ) [8]. The spectral reflectance of the surface F is reported by Konttinen et al. [8]. Optical microscopy (Fig. 2) revealed that the surface is inhomogeneously covered by a dark substance, which has been identified as carbon [8]. Additionally, different shades of dark are visible. An XPS analysis confirmed that carbon on the surface is mainly in graphite form (see Section 3.2 for details).

Graphite seems to be clustered in some areas, whereas in other areas uncovered  $Al_2O_3$  is visible. This phenomenon can be explained with the nature of the manufacturing process: the hard silicon carbide particles scratch grooves onto the surface, thus mechanically introducing carbon dust to the revealed pure Al surface. Some of the carbon is adsorbed onto the grooves thus forming a seed for a graphite cluster to be agglomerated. While the grinding process continues, the silicon carbide particles begin to remove agglomerated graphite from some areas, by introducing new grooves on top of the earlier ones. A clear example of this can be seen in Fig. 2 (100 $\times$  magnification), where a wide scratch has

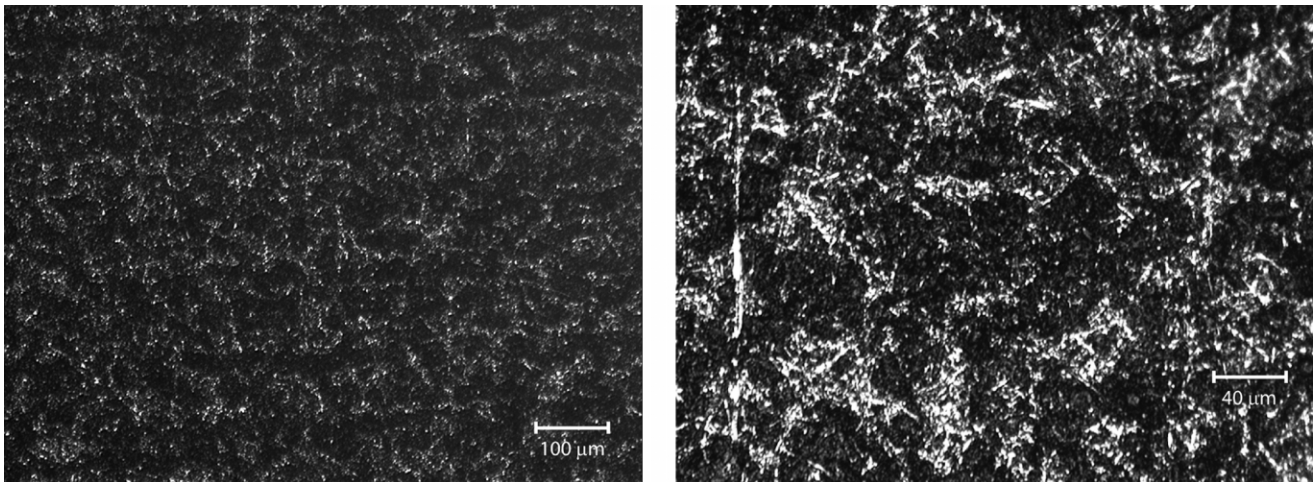


Fig. 2. Optical photograph of the surface F, 40× (left) and 100× (right) magnification.

revealed the  $\text{Al}_2\text{O}_3$  substrate. In addition, the combination of the grinding pads and the grinding parameters applied so far does not seem to allow a homogeneous groove structure to be formed on the surface. Therefore graphite agglomeration does not occur throughout the surface.

### 3.2. XPS analysis

Two samples of surface F were analysed by XPS. The results are shown in Fig. 3, the two samples are

denoted as 1 and 2. The peak intensities of the binding energies are approximately 74.3 eV ( $\text{Al}2p$ ), 284.8 eV ( $\text{C}1s$ ) and 531.5 eV ( $\text{O}1s$ ). In literature,  $\text{Al}2p$  with 74.3 eV [10] and 74.35 eV [11] as well as  $\text{O}1s$  with 531.52 eV [12] are related to  $\text{Al}_2\text{O}_3$ . This was expected, as aluminium oxidizes naturally in air forming a thin  $\text{Al}_2\text{O}_3$  layer on Al substrate.

The  $\text{C}1s$  compound corresponding to the peak binding energy of 284.8 eV is more complicated to resolve. Carbon compounds were expected based on earlier EDS analysis, which revealed elements Al and O, with small

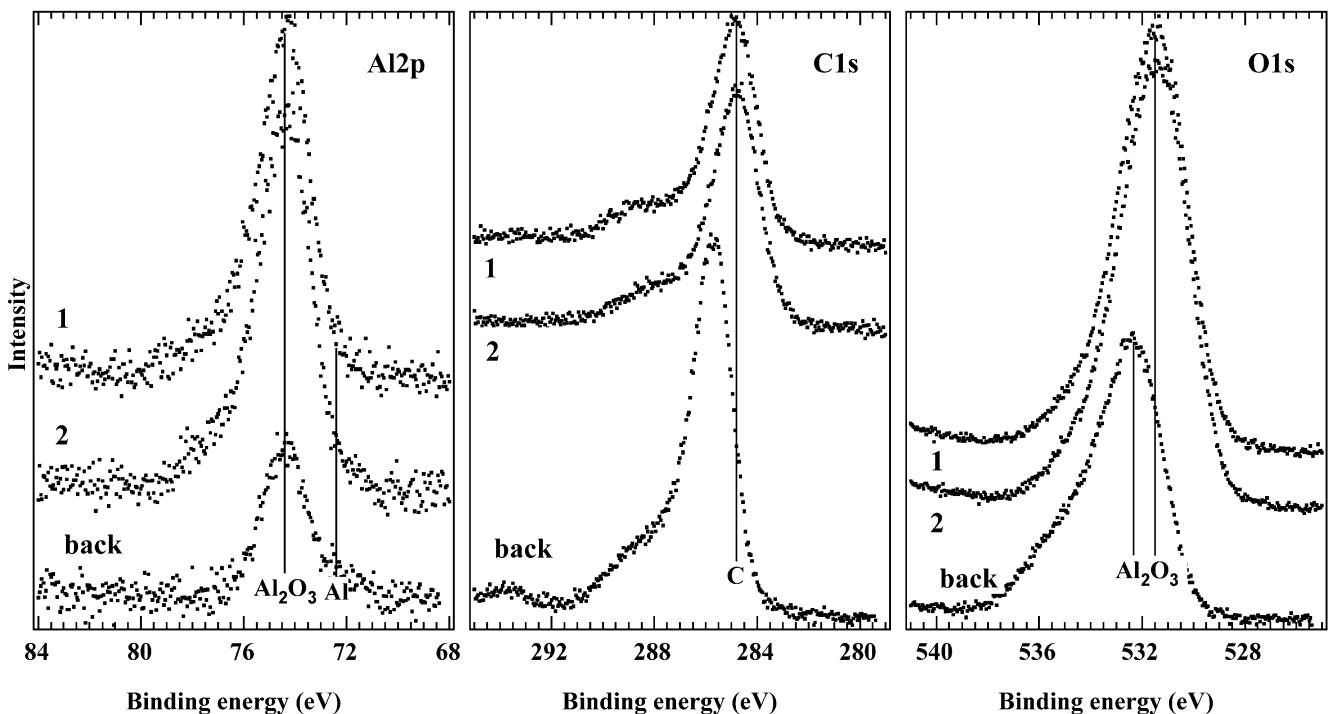


Fig. 3. XPS analysis of two samples of the surface F, denoted as 1 and 2 and backside of the surface F denoted as 'back'. Corresponding peak intensity binding energies of samples 1 and 2 are related to  $\text{Al}_2\text{O}_3$  (74.35 and 531.52 eV) and C in graphite form (284.8 eV).

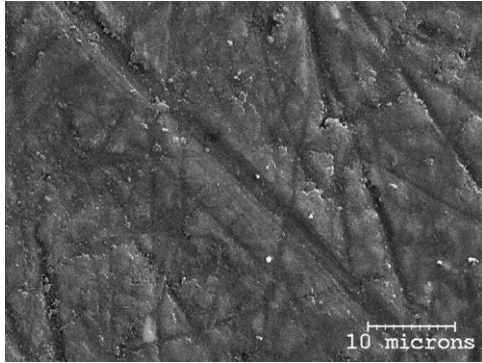


Fig. 4. SEM photograph of a typical surface sample, 2000 $\times$  magnification.

traces of C, Si, Au, Mn, Fe and Cu [8]. However, 1313 matches were found for C1s [13]. Of these, 81 matches to the binding energy of 284.8 eV. All but one of the 81 matches can be discarded due to presence of other elements than those detected by the EDS. Based on the EDS and XPS analyses, the only possible match is carbon in graphite form [14]. Based on the optical microscopy analysis it is most likely that the grinding process mechanically incorporates adsorbed and agglomerated graphite onto the surface. The carbon matrix structure in turn is composed of agglomerated graphite clusters.

Although the grinding process is done in room temperature it is speculated that due to abrasive forces the local temperature of the active grinding particle and the corresponding part of the substrate surface would very briefly and momentarily rise up to several hundreds degrees Celsius. Due to measuring difficulties this has not been verified. Some other potential C1s matches (such as HC=O, CO, (CH<sub>2</sub>)<sub>n</sub>, CHO, not marked in Fig. 3) with smaller binding energy intensities could have been formed.

In addition, the backside of a sample of surface F was analysed, denoted as 'back' in Fig. 3. Due to the nature of the manufacturing method containing carbon dust, the backside of the substrate is contaminated with carbon compounds while attached to the grinding bed. Different peak energies for O1s were measured for backside (532.3 eV, related to Al<sub>2</sub>O<sub>3</sub> [15]) compared to the samples 1 and 2. There are two possible reasons for this: the energy scale was fixed to Al2p for all samples (assuming Al<sub>2</sub>O<sub>3</sub> would be found) and C1s and O1s peak intensities were gained as a result. This could have caused some displacement for C1s and O1s results. Secondly, exact peak binding energies varied slightly between measurements.

### 3.3. Crosscut SEM and EDS analyses

Figs. 4 and 5 show top and cross-cut SEM photographs of typical absorber surface samples. In Fig. 4

approximately 1–2  $\mu$ m wide microgrooves can be seen on top of the surface, similar to those reported by Konttinen et al. [8,9]. The sample in Fig. 5 was manufactured by diamond polishing of a cross-section of a plastic-embedded surface: a sample of a surface was placed in between two pieces of stainless steel (SS) and cast in epoxy. The sample was sawed in half and the cross-cut section was manually diamond-polished as smooth as possible.

Visible in Fig. 5 (just below the surface borderline) are light colour areas (denoted as 3), which can be interpreted as clustered graphite adsorbed and agglomerated on the microgrooves of the Al<sub>2</sub>O<sub>3</sub> surface. The maximum visible carbon cluster thickness is approximately 300 nm. Another spot of the same sample was examined by an EDS analysis to verify the composition of the light areas as graphite. A large amount of C was found, but significant amounts of O and Al were identified as well. Similarly, areas positively known as Al and Fe contained lesser, but still significant amount of C [16]. The most likely explanation for this is that the cross-cut sample becomes contaminated during the diamond polishing with all the elements present on the surface. Therefore it was not possible to positively identify the composition of the light areas as graphite with the EDS.

Utmost care was taken to make the surface borderline between the SS and the C/Al<sub>2</sub>O<sub>3</sub>/Al-layers as sharp as possible. Three samples were manufactured with this method, the sample shown in Fig. 5 being the best of them. However, as can be seen in Fig. 5, some SS has possibly yielded on top of the C/Al<sub>2</sub>O<sub>3</sub>/Al-layer during

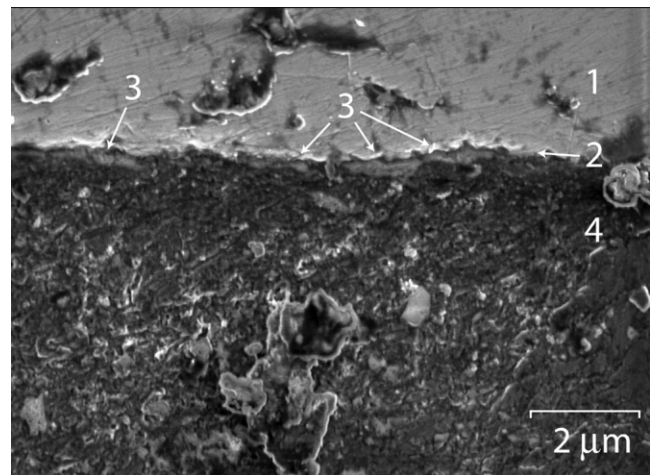


Fig. 5. A cross-cut SEM photograph of a typical surface sample, 10 000 $\times$  magnification. (1) Stainless steel (SS) attached on top of the surface before crosscutting, (2) surface borderline between the SS and Al<sub>2</sub>O<sub>3</sub> layers, active absorber surface facing up, (3) areas interpreted as graphite clusters adsorbed and agglomerated on the microgrooves of the Al<sub>2</sub>O<sub>3</sub> surface, maximum visible cluster thickness 300 nm, (4) Al substrate.

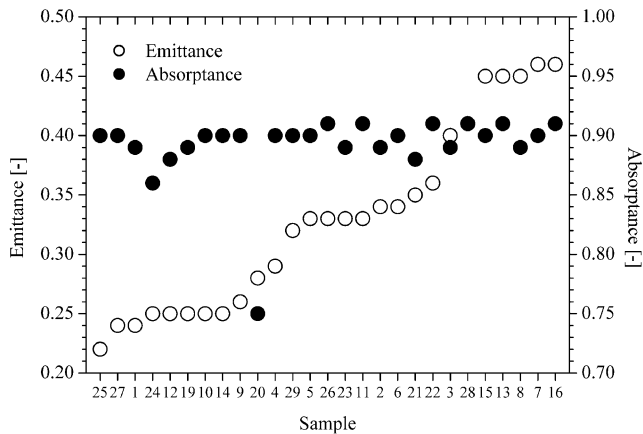


Fig. 6. Solar absorptance (AM1.5) and thermal emittance (100 °C) of 27 experimental samples manufactured with different grinding parameters (grinding speed, number of grinding sequences and additional grinding weight), smallest emittance on the left (samples 17–18 omitted due to poor quality).

the diamond polishing, thus increasing the uncertainty of the analysis of the thickness and the width of the visible components.

#### 4. Analysis of relation between graphite coverage and optical properties of the surface

In the past few years, hundreds of C/Al<sub>2</sub>O<sub>3</sub>/Al absorber samples with altering manufacturing parameters have been characterized. The graphite coverage seems to dominate the absorption of the surface, since no absorptance higher than 0.91 have been achieved so far. If the surface would be covered by a homogeneous graphite layer thick enough, the solar absorptance would be  $\geq 0.94$  [17]. In order to find the manufacturing parameters, which would maximize  $\alpha$ , 27 experimental

samples were manufactured. The parameters changed in the manufacturing process were grinding speed (relative units between 1 and 10), grinding sequences (between 8 and 14) and additional weight added on top of grinding unit (from 0 to 4.5 kg). Fig. 6 shows  $\alpha$  and  $\varepsilon$  of these samples. Most of these surfaces have  $\alpha$  over 0.88 and  $\varepsilon$  higher than 0.25. The optical measurement equipment used at Helsinki University of Technology (HUT) is reported by Konttinen et al. [8].

Figs. 7 and 8 show optical photographs of the samples with the smallest (25) and the highest (16) emittance. The photographs were taken with exactly the same microscope parameters with high brightness in order to enhance contrast between the dark and the light areas.  $\alpha$  of the samples 25 and 16 is 0.90 and 0.91 and  $\varepsilon$  is 0.22 and 0.46, respectively. The experimental manufacturing parameters for the sample 25 were: relative grinding speed 10, 11 grinding sequences and additional weight of 3.15 kg. For sample 16 the values were: relative grinding speed 5, 12 grinding sequences and additional weight of 3.6 kg. In addition, sample 25 only was heated up moderately during the grinding (actual temperature not measured). Almost equal optical properties were gained without heating (sample 27,  $\alpha = 0.90$ ,  $\varepsilon = 0.24$ ). As can be seen by comparing the Figs. 7 and 8 (both 40 $\times$  and 100 $\times$  magnification), the surface of the sample 16 appears significantly darker than the surface of the sample 25. In addition, the visible graphite coverage is larger for the sample 16.

Fig. 9 shows the luminosity distribution of the samples 25 and 16 (100 $\times$  magnification), respectively. The scale is from 0 (black) to 255 (white). The surface 16 has smaller mean and median values, thus indicating a darker surface. The luminosity distribution of 16 is significantly more biased towards dark as well. Although it is not possible to directly determine the thickness of

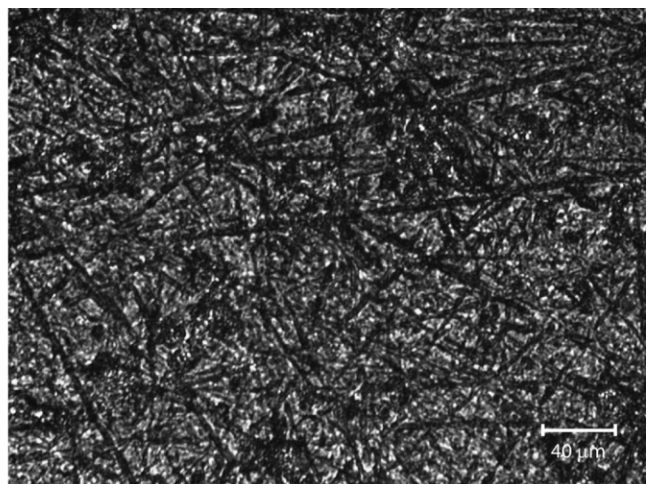
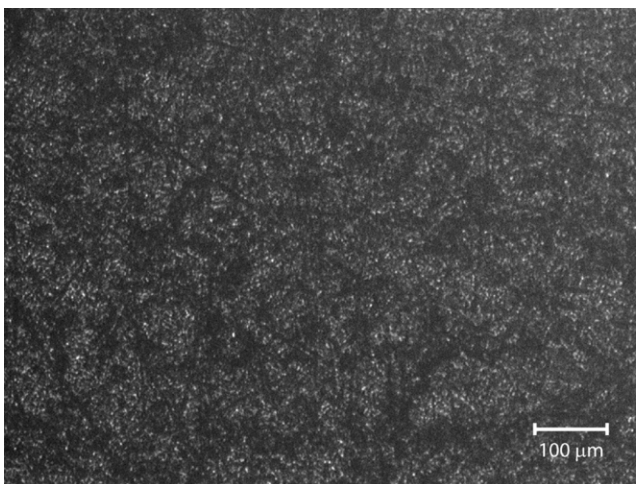


Fig. 7. Optical photograph of the surface 25, 40 $\times$  (left) and 100 $\times$  (right) magnification.

the graphite layer from Figs. 7–9, it is most likely that the surface of the sample 16 is significantly thicker compared to 25, thus resulting in  $\varepsilon$  more than doubled.

However, the graphite coverage difference between 25 and 16 has almost no effect on  $\alpha$ . The thicker graphite layer of the sample 16 does not compensate for the missing graphite coverage, and therefore  $\alpha$  does not rise above 0.91 even for the samples with the highest  $\varepsilon$ . Based on all samples characterized earlier and these results it can be concluded that the graphite coverage of the sample 25 is as good as can be achieved for the grinding method used so far, with the lowest emittance achieved. Altering the composition of the grinding pad and finding the best grinding parameters for the enhanced pad could result in more homogeneous graphite coverage and higher  $\alpha$ . If the thickness of the graphite layer could be reduced  $\varepsilon$  would become lower as well. Different material compositions, grain sizes and grain density are to be tested in the future to that end.

An interesting question is: does the surface act as an optical trapping device? Optical trapping occurs by reflective and resonant scattering. Reflective scattering is obtained purely by the geometry of the surface. According to Lampert [18], for particulate coatings a resonant scattering deals with both the size and optical properties of the particles and the surrounding media. The Mie effect and Maxwell-Garnett theory predict high forward scattering from particles much less than 0.10 of the wavelength of the incident energy. In the SEM photographs (Fig. 4, also Figures 3–4 in Konttinen et al. [8]) the width of the visible grooves is between 1 and 2  $\mu\text{m}$ . The distance between microgrooves varies and is never exactly the same between any given spots on a surface. In any case the whole surface is not evenly and thoroughly covered with the microgrooves and graphite clusters. Taking into account the size of the microgrooves and graphite clusters and their coverage,

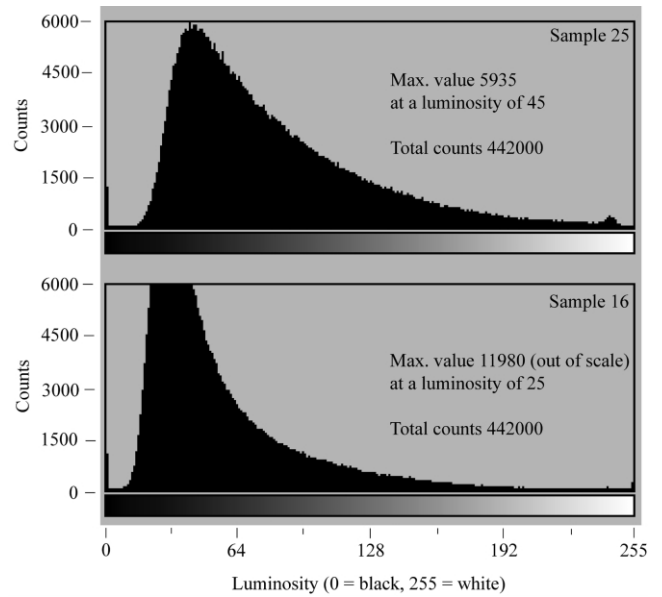


Fig. 9. Luminosity of the surfaces 25 (top) and 16 (bottom), scale from 0 (black) to white (255),  $100\times$  magnification. Corresponding values for sample 25: mean 79, median 67 and for sample 16: mean 54, median 40.

it is unlikely that optical trapping contributes to a large extent to the absorptance of the surface.

## 5. Conclusions

It has been shown that the mechanically manufactured C/Al<sub>2</sub>O<sub>3</sub>/Al selective surface contains a matrix surface structure consisting of agglomerated graphite clusters and Al<sub>2</sub>O<sub>3</sub> substrate. Micronic carbon is adsorbed on the surface thus forming a seed for the graphite clusters to be agglomerated. With the current grinding method the resulting surface is not evenly and homogeneously

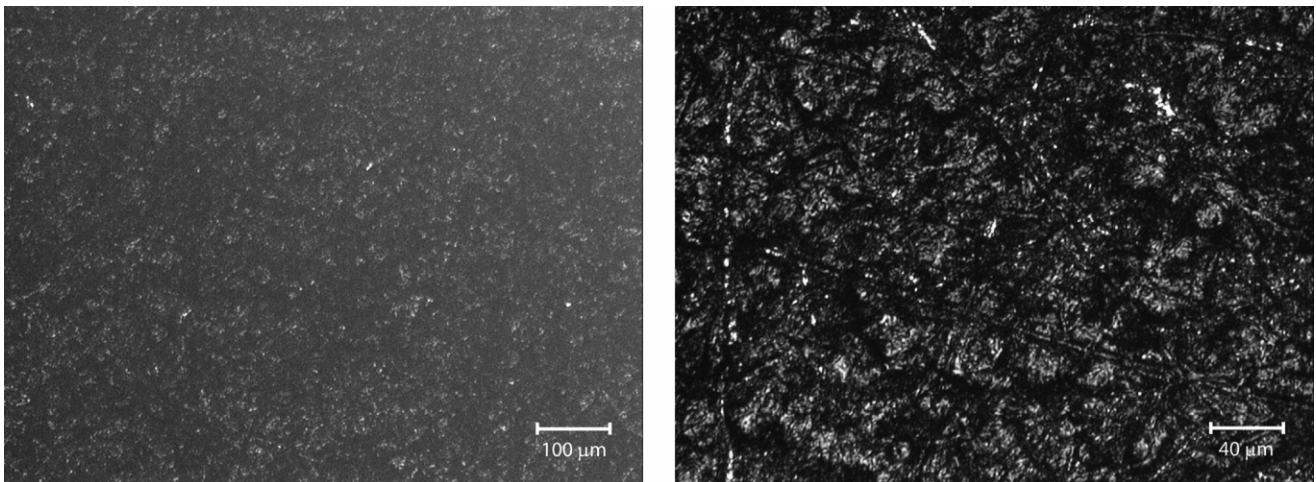


Fig. 8. Optical photograph of the surface 16,  $40\times$  (left) and  $100\times$  (right) magnification.

covered by the graphite, thus resulting in  $\alpha \leq 0.91$ . Altering the composition of the grinding pad and locating the best grinding parameters for the advanced pad could result in a higher  $\alpha$  as the graphite coverage could be increased. In the optimal case,  $\alpha \geq 0.94$  could be achieved.

The maximum graphite cluster thickness is determined to be in the range of 300 nm for a surface having  $\alpha = 0.88$  and  $\varepsilon = 0.27$ . Increasing  $\alpha$  of a surface to a level of 0.90–0.91 resulted in  $\varepsilon$  of 0.22–0.46, thus indicating that very small changes in the grinding process (resulting in thicker graphite layer) can increase  $\varepsilon$  significantly with almost no effect on  $\alpha$ . The luminosity distribution of a surface with  $\varepsilon = 0.47$  is significantly more biased towards dark compared to a surface with  $\varepsilon = 0.22$ . However,  $\alpha$  of these samples is almost the same (0.91 and 0.90, respectively), thus indicating that with an optimized grinding method  $\varepsilon$  could be reduced by decreasing the graphite thickness.

### Acknowledgments

Financial support from the National Technology Agency of Finland (Tekes) is gratefully acknowledged. We would also like to thank Mr Jukka Paatero at HUT for his support in identifying the graphite structure on the surface and Dr Unto Tapper and Mr Tom E. Gustafsson from Technical Research Centre of Finland (VTT) for SEM and EDS analyses. Mr Mika Kolari from VTT manufactured the cross section samples, and Prof. Jouko Lahtinen from HUT conducted the XPS analysis.

### References

- [1] M. Farooq, M.G. Hutchins, *Sol. Energy Mater. Sol. Cells* 71 (2002) 523.
- [2] E. Wäckelgård, G. Hultmark, *Sol. Energy Mater. Sol. Cells* 54 (1998) 165.
- [3] Q.C. Zhang, *Sol. Energy Mater. Sol. Cells* 52 (1998) 95.
- [4] T. Eisenhammer, A. Mahr, A. Haugeneder, W. Assmann, *Sol. Energy Mater. Sol. Cells* 46 (1997) 53.
- [5] Z. Orel, M.K. Gunde, *Sol. Energy Mater. Sol. Cells* 68 (2001) 337.
- [6] M.K. Gunde, J.K. Logar, Z.C. Orel, B. Orel, *Thin Solid Films* 277 (1996) 185.
- [7] M.D. Kudryashova, *Appl. Sol. Energy* 5 (1969) 24.
- [8] P. Konttinen, P.D. Lund, R. Kilpi, Mechanically manufactured selective solar absorber surfaces, *Sol. Energy Mater. Sol. Cell*, in press.
- [9] P. Konttinen, Lic.Sc. Thesis, Department of Engineering Physics and Mathematics, Helsinki University of Technology, Finland, 2000.
- [10] E. Paparazzo, *Surf. Interface Anal.* 12 (1988) 115.
- [11] V.I. Nefedov, *J. Electron Spectrosc. Relat. Phenom.* 25 (1982) 29.
- [12] C.D. Wagner, D.E. Passoja, H.F. Hillary, T.G. Kinisky, H.A. Six, W.T. Jansen, J.A. Taylor, *J. Vac. Sci. Technol.* 21 (1982) 933.
- [13] NIST X-ray Photoelectron Spectroscopy Database, NIST Standard Reference Database 20, Version 3.2 (Web Version), available at <http://srdata.nist.gov/xps>, February 12, 2002.
- [14] B.J. Bachman, M.J. Vasile, *J. Vac. Sci. Technol. A* 7 (1989) 2709.
- [15] K. Kishi, S. Ikeda, *Bull. Chem. Soc. Jpn.* 46 (1973) 341.
- [16] P. Konttinen, P.D. Lund, in: *Proceedings of World Renewable Energy Congress VII*, Cologne, Germany, 29 June–5 July, 2002.
- [17] J.A. Duffie, W.A. Beckman, *Solar Engineering of Thermal Processes*, second ed., Wiley Interscience, New York, 1991.
- [18] C.M. Lampert, *Sol. Energy Mater.* 1 (1979) 319.